Nile Red-Based GPCR Ligands as Ultrasensitive Probes of the Local Lipid Microenvironment of the Receptor

Fabien Hanser, Claire Marsol, Christel Valencia, Pascal Villa, Andrey S. Klymchenko, Dominique Bonnet*# and Iuliia A. Karpenko*#

Abstract: The local lipid microenvironment of transmembrane receptors is an essential factor in G-protein coupled receptor (GPCR) signaling. However, tools are currently missing for studying endogenously expressed GPCRs in primary cells and tissues. Here we introduce fluorescent environment-sensitive GPCR ligands for probing the microenvironment of the receptor in living cells using fluorescence microscopy under no-wash conditions. We designed and synthesized antagonist ligands of the oxytocin receptor (OTR) by conjugating a high-affinity non-peptidic OTR ligand PF-3274167 to the environment-sensitive fluorescent dye Nile Red. The length of the polar PEG spacer between the pharmacophore and the fluorophore was adjusted to lower the non-specific interactions of the probe while preserving a strong fluorogenic response. We demonstrated that the new probes embed into the lipid bilayer in the vicinity of the receptor and convey the information about the local polarity and the lipid order via the wavelength-shifting emission of the Nile Red fluorophore.

INTRODUCTION

G-protein coupled receptors (GPCRs) are a superfamily of transmembrane receptor proteins that are ubiquitously expressed in the human body and widely involved in human physiology and pathophysiology. GPCRs represent the most intensively studied targets for small-molecule therapeutics. For instance, more than 470 (> 30%) of currently marketed drugs act on over a hundred of unique GPCRs, with hundreds of prospective drugs being in preclinical development and clinical trials.[1–4] The field of GPCR research had been boosted by the recent breakthrough in the structural biology of transmembrane receptors, which revealed the three-dimensional architecture and conformational dynamics of isolated receptors, receptor–ligand and receptor–transducer protein complexes at an unprecedented atomic-level resolution. These findings gave numerous structural insights into the selectivity of ligand recognition and mechanisms of the signal transduction, facilitating further biochemical and pharmacological exploration of this class of drug targets.[5–7] Although these advances have opened new avenues for the rational development of GPCR-targeting drugs, we still have only a dim understanding of the GPCR activation and signal transduction in the complex cellular context. GPCRs are embedded into highly heterogeneous and dynamic cellular membranes, where lipid organization and the presence of lipid nanodomains[8,9] can modulate the functioning of the receptor. To fill the gap between the growing body of structural information obtained on purified receptors *ex vivo*[10] and understanding their functioning and the heterogeneity of signaling in living cells, a multitude of chemical, pharmacological and optical tools has been developed.[11–15] Fluorescence-based methods are of particular interest for studying GPCR in their native environment because of their high sensitivity, high spatial and temporal resolution and possibility to apply them in intact living cells and tissues.[16,17] Besides that, the key advantage of fluorescence sensing is the possibility to directly and site-specifically probe dynamic molecular interactions using environment-sensitive small-molecule fluorescent reporters.[18,19]

Local alterations of the lipid microenvironment, such as the presence of highly organized lipid nanodomains, known as lipid rafts, can affect the conformation equilibrium of the transmembrane receptor, its affinity to ligands and its protein-protein interactions.[20–25] Therefore, studying the lipid microenvironment of receptors is of fundamental importance for understanding and modulating GPCR signaling.[26] However, the progress has been hampered by the lack of reliable experimental methods and by the multiple controversies related to the lipid raft hypothesis.[27] Environment-sensitive probes, such as LAURDAN,[28] di-4-ANEPPDHQ,[29] Nile Red (NR) derivatives,[30,31] could be used to address the lipid order in biomembranes through shifts in the emission color.[32] However, these probes report the average lipid order of the bulk of cell membrane and are not suitable for probing specifically the receptor microenvironment. One work addressed probing of the local receptor microenvironment within the Förster radius by using time-resolved FRET from a GLP-1 receptor labeled with a long-life luminescent terbium cryptate to NR-based probe NR12S.[33] However, studying the local lipid microenvironment of untagged GPCRs in intact living cells and tissues remains a formidable challenge. In our previous works, we synthesized optically-responsive chemical probes targeting the oxytocin receptor (OTR), a class A GPCR. In our design, a peptidic agonist of the receptor was covalently tethered to the NR fluorophore, known for its strong solvatochromism and fluorescence in the orange-red spectral region.[34] The resulting conjugate delivered the fluorescent probe directly into the lipid bilayer in the vicinity of the receptor. Being non-fluorescent in water, the conjugate displayed a strong enhancement of fluorescence upon binding to the receptor, enabling qualitative and quantitative detection of the receptor under wash-free conditions. Although the solvatochromic properties of Nile Red have been successfully used for probing the polarity and molecular organization of biological membranes,[30,31,35,36] the utility of our first-generation OTR-targeting fluorescent probes for studying the lipid microenvironment of the native receptors was limited because of their agonism. Binding of the probes to the OTR triggered fast cellular response resulting in the rapid internalization of the receptor which is usually associated with the dramatic changes of lipid composition of the receptor within the endosomal compartment. In the present work, we address these limitations and report a new generation of GPCR-targeting fluorescent probes. To overcome the problem of receptor internalization, we designed, synthesized and characterized a series of antagonist-based conjugate delivering the environment-sensitive fluorogenic Nile Red-based probe into the vicinity of the OTR. We used a combination of steady-state fluorescence spectroscopy and ratiometric confocal fluorescence microscopy to demonstrate the ability of the new probes to embed into the lipid bilayer in the vicinity of the receptor in living cells and to transmit the information about the properties of the local lipid microenvironment via the color-shifting emission of the NR fluorophore.

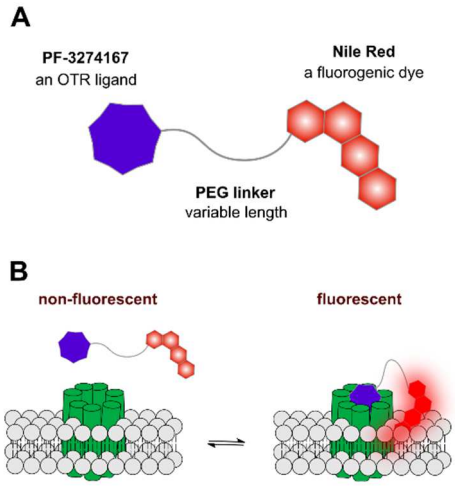

Figure 1. The design (a) and the working principle (b) of the fluorogenic non-peptidic OTR ligands.

RESULTS AND DISCUSSION

Design and Synthesis. To design antagonist-based environment-sensitive conjugates targeting the OTR we used the approach that had been validated on peptidic OTR agonists.[34] Solvatochromic fluorogenic NR dye was covalently tethered to a non-peptidic antagonist of the OTR via a flexible linker of variable length (Figure 1A). NR-based carboxylic acid NR-COOH (**4**, Scheme 1) and the desmethyl precursor of the OTR-selective antagonist PF-3274167[37,38] were chosen as the key structural blocks to be conjugated through a flexible polyethylenglycol (PEG)-based tethers of variable length. Four PEG linkers composed of 4 – 20 ethylenic moieties were selected and tested to decrease the off-target binding of the probes and to finely tune the specificity of the probe and its fluorogenic response upon homogenous wash-free imaging condition (Figure 1B). First, we revised the synthesis of NR-COOH **4** (Scheme 1). The procedure reported in the literature starts from the conversion of commercially available 3-diethylaminophenol **1** into nitrosophenol **2**, which is then engaged into an intermolecular oxidative cyclization with 1,6-dihydroxynaphthalene to give the phenol derivative of Nile Red **3.** According to the original protocols,[39,40] nitrosophenol **2** was purified by recrystallization from ethanol/diethyl ether mixture and then refluxed in DMF with 1,6-dihydroxynaphthalene to give the desired compound **3** in moderate yield of 42% over two steps.

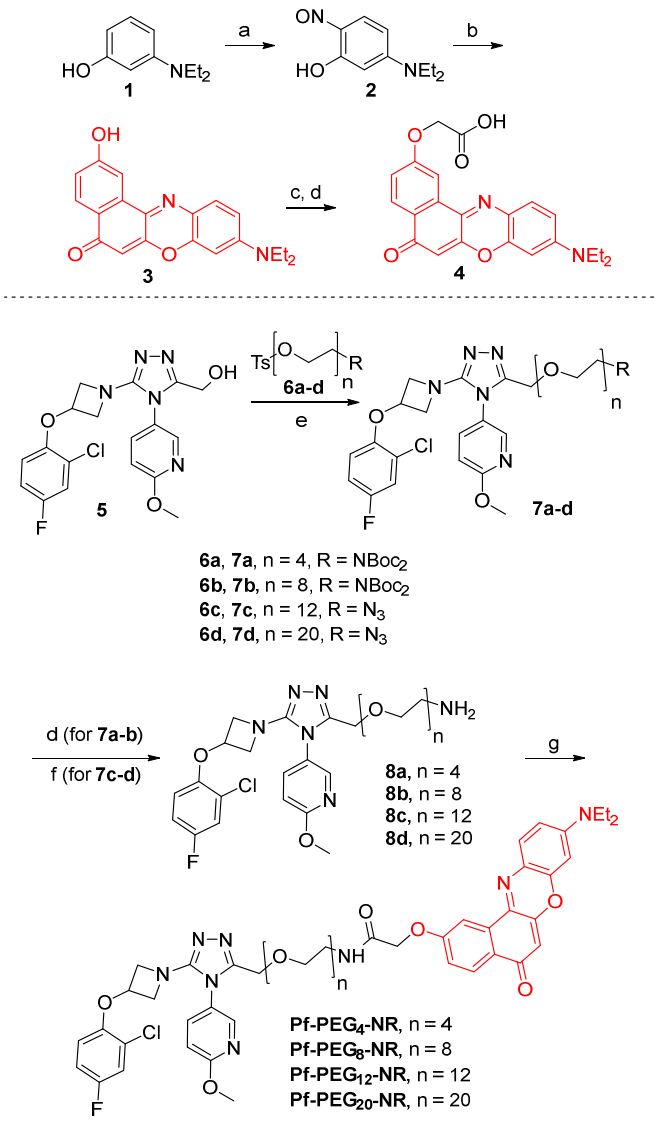

Scheme 1. Synthesis of the non-peptidic fluorescent OTR ligands. a) $NaNO_2$, HCl, H_2O, 0 °C, 2.5 h. b) 1,6-Dihydroxynaphthalene, DMF, 110 °C, 45 min. c) *tert*-Butyl chloroacetate, K_2CO_3, acetone, reflux, 6.5 h. d) Trifluoroacetic acid, DCM, 25 °C, 0.5–3.5 h. e) KOH, DMF, 0–45 °C, 2.5–67 h. f) Triphenylphosphine polymer-bound, THF, reflux then H_2O, reflux, 5–7 h. g) **4**, PyBOP, DIPEA, DMF, 25 °C, 0.5–25 h..

However, in our hands the recrystallization of nitrosophenol **2** was not robustly reproducible. To make things worse, nitrosophenol was found to decompose upon boiling in DMF, resulting in highly variable and significantly lower yields of Nile Red derivative **3** (27% at best). We improved the synthetic protocol by omitting the problematic crystallization step. We found that better yields of **3** were obtained when the crude nitrosophenol **2** was isolated by evaporation of the acidic reaction mixture and engaged into the cyclization without further purification. The intermolecular cyclization was carried out with 2 equiv. of nitrosophenol **2** in DMF at 110 °C for 45 min. Following the proposed protocol, the phenol derivative of Nile Red **3** was obtained in 44% yield over two steps. The protocol was robustly reproducible on 0.45 – 3 mmol scale. Phenol **3** was then alkylated with *tert*-butyl chloroacetate[41] and then *tert*-butyl protecting group was removed by the treatment with trifluoroacetic acid to afford NR-COOH **4** in 84% yield over two steps (Scheme 1).

The synthesis of the desmethyl precursor of PF-3274167 **5** and its two pegylated derivatives **8a** and **8b** bearing PEG_4 and PEG_8 chains (Scheme 1) was performed following our previously established protocols.[38] Regarding PEG_{12} and PEG_{20} derivatives **8c** and **8d**, we found it more convenient to synthesize these amines by reducing the corresponding azides. To achieve this, we first alkylated the desmethyl precursor of PF-3274167 **5** with azido-tosylates **6c** and **6d** in the presence of KOH in DMF affording pegylated triazoles **7c** and **7d** in 92% and 72% yield, respectively. Next, **7c** and **7d** were converted into amines **8c** and **8d** using the Staudinger reduction in the presence of polymer-bound triphenylphosphine. Finally, coupling of amines **8a-d** to NR-COOH **4** led to the formation of the desired OTR non-peptidic ligands Pf-PEG_4-NR, Pf-PEG_8-NR, Pf-PEG_{12}-NR and Pf-PEG_{20}-NR.

Spectroscopic Characterization. The fluorescence properties of the Nile Red derivatives were first studies in a series of solvents of different polarity. Steady-state fluorescence spectra of the OTR ligands (Figure 2A) revealed that the strong solvatochromic and fluorogenic character of Nile Red was retained upon conjugation of NR-COOH to the OTR ligand via the PEG linkers. All the four OTR ligands were highly fluorescent in apolar solvents such as 1,4-dioxane with the emission maxima of about 585 nm (Table 1). Due to the positive solvatochromism of Nile Red, the emission maxima in water bathochromically shifted to 660 nm, and the fluorescence quantum yields gradually decreased with the increasing polarity of the solvent.

Table 1. Fluorescence properties of NR and the NR conjugates

Solvent	NR			NR conjugates					
	λ_{max}, nm		QY[c]	λ_{max}, nm		QY[c]			
	abs[a]	fluor[b]		abs[a]	fluor[b]	Pf-PEG_4-NR	Pf-PEG_8-NR	Pf-PEG_{12}-NR	Pf-PEG_{20}-NR
1,4-Dioxane	520	581	0.70	521[d]	584[d]	0.65	0.65	0.67	0.68
Acetone	533	612	0.68	534[d]	612[d]	0.65	0.64	0.65	0.66
Acetonitrile	535	618	0.65	538[d]	619[d]	0.62	0.60	0.63	0.65
Ethanol	549	634	0.51	551[d]	634[d]	0.48	0.48	0.51	0.52
Methanol	553	640	0.38	556[d]	639[d]	0.37	0.38	0.39	0.41
Water	593	663	0.05	601[d]	661[d]	0.07	0.10	0.11	0.11

[a] Position of the absorption maximum. [b] Position of the emission maximum. [c] Fluorescence quantum yield. [d] Similar values (+/- 2 nm) were observed for all the four conjugates.

An important parameter for cellular studies upon wash-free conditions is the fluorescence turn-on ratio, a quantitative measure of the fluorogenic properties of the probes. Here we define it as the ratio of the

fluorescence intensity at 620 nm in an apolar solvent (1,4-dioxane) to that in water. All the four NR conjugates demonstrated excellent fluorogenic properties with relative turn-on ratios ranging from 18- to 35-fold (Figure 2B).

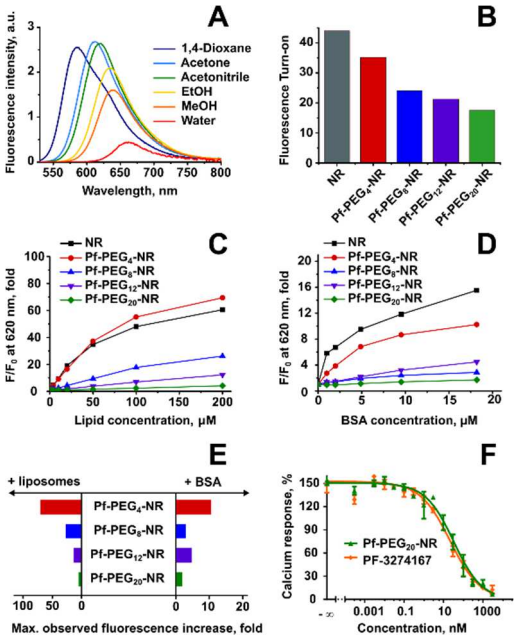

Figure 2. Fluorescence and pharmacological properties of the OTR ligands. a) Fluorescence spectra of Pf-PEG$_4$-NR in different solvents. Fluorescence intensity is normalized to the absorbance at 520 nm. b) Fluorogenic properties of Nile Red (NR) and the OTR fluorescent ligands. The relative fluorescence turn-on was calculated as a ratio of the fluorescence intensity at 620 nm in 1,4-dioxane (normalized to the absorbance at 520 nm) to that in water (normalized to the absorbance at 520 nm). c) Evaluation of non-specific interactions of the OTR ligands and NR with DOPC/cholesterol (2:1) liposomes: fluorescence intensity increase at 620 nm (F/F0) as a function of liposomes concentration in PBS. d) Evaluation of non-specific interactions of the OTR ligands and NR with BSA: fluorescence intensity increase at 620 nm (F/F0) as a function of BSA concentration in PBS. e) Maximal observed fluorescence increase due to non-specific interactions of the OTR ligands with liposomes and BSA. f) Representative dose-response curves for OTR antagonists PF-3274167 and Pf-PEG$_{20}$-NR. Values are means ± SEM.

Evaluation of Non-Specific Interactions. In the development of fluorescent probes for live-cell studies of membrane receptors it is crucial to carefully evaluate the non-specific interactions of the probes with cellular membranes and serum proteins. To address this issue, we used 1,2-dioleoyl-sn-glycero-3-phosphocholine (DOPC) / cholesterol (2:1) large unilamellar vesicules (LUVs) as a model of cell membranes and BSA to evaluate the binding to plasma proteins. Nile Red is known for its strong non-specific binding to lipid membranes,[42] lipid droplets[43] and hydrophobic protein pockets.[44–46] In our hands, fluorescence of Nile Red (Figures 2C and 2D, black line) did gradually increase upon addition of liposomes or BSA to its aqueous solution. The NR conjugates were evaluated under the same conditions. As we expected based on our previous work with the OTR agonists, the increase of the length of the polar PEG spacer resulted in a gradual decrease of the non-specific interactions (Figure 2E). For instance, Pf-PEG$_4$-NR bound to the liposomes with similar affinity to Nile Red. Its interaction with BSA was less pronounced comparing to unmodified Nile Red but still significant, making this probe poorly compatible with the live-cells imaging conditions. Although Pf-PEG$_8$-NR and Pf-PEG$_{12}$-NR did not

display significant binding to BSA, they were still strongly interacting with model membranes. Finally, the non-specific binding to lipid membranes and BSA became almost negligible for Pf-PEG_{20}-NR, making this ligand the most promising for cellular studies of the OTR.

Functional Characterization. In order to verify whether the introduction of PEG spacers influenced the functional activity of the PF-3274167 pharmacophore, we measured its effect on the calcium response in HEK 293 cells stably overexpressing the OTR (HEK-OTR cells). Both the unmodified PF-3274167 and the most promising probe Pf-PEG_{20}-NR fully inhibited the oxytocin-induced calcium accumulation in a dose-dependent manner with similar IC_{50} of 15 ± 3 nM and 30 ± 3 nM, respectively, highlighting the antagonist character of both ligands (Figure 2F). As for the ligands with the PEG chains of 4, 8 and 12, they also displayed antagonist character with slightly lower potency (132 nM, 92 nM and 83 nM, respectively), which could be explained by non-specific binding to cellular membranes or to BSA present in the buffer (Supplementary Table S1 and Supplementary Figure S2). To conclude, the introduction of a cumbersome PEG spacers capped with the aromatic fluorophore has a low impact on the functional activity of the ligand which retained its antagonist character.

Wash-Free Imaging of the OTR in Living Cells. Next, the confocal microscopy study on living HEK-OTR cells was performed in order to evaluate the ability of the developed probes to detect the receptor under wash-free conditions. We were pleased to find that Pf-PEG_{20}-NR, the conjugate having the most favorable combination of properties in the non-specific binding assay, showed exclusive localization on the plasma membrane, whereas no cytotoxicity was observed (Supplementary Figure S3). Importantly, the OTR retained on the cell membrane with no detectable ligand-induced internalization, due to the antagonist character of PF-3274167 (Figure 3). A competition assay was then used to demonstrate the specificity of the probe towards the OTR. Indeed, upon addition of a large excess of a non-fluorescent OTR-binding competitor carbetocin (CBT), the plasma membrane signal disappeared, indicating that Pf-PEG_{20}-NR binds to the cell reversibly in a receptor-specific manner. We also confirmed by confocal microscopy that the ligands with the PEG chains of 4, 8 and 12 units exhibited a strong non-specific binding, as one would have expected from the *in vitro* non-specific binding assay (Figure 2C-E). Their fluorescence was not influenced by the addition of the non-fluorescent competitor and, moreover, these ligands rapidly crossed the plasma membrane and stained intracellular structures.

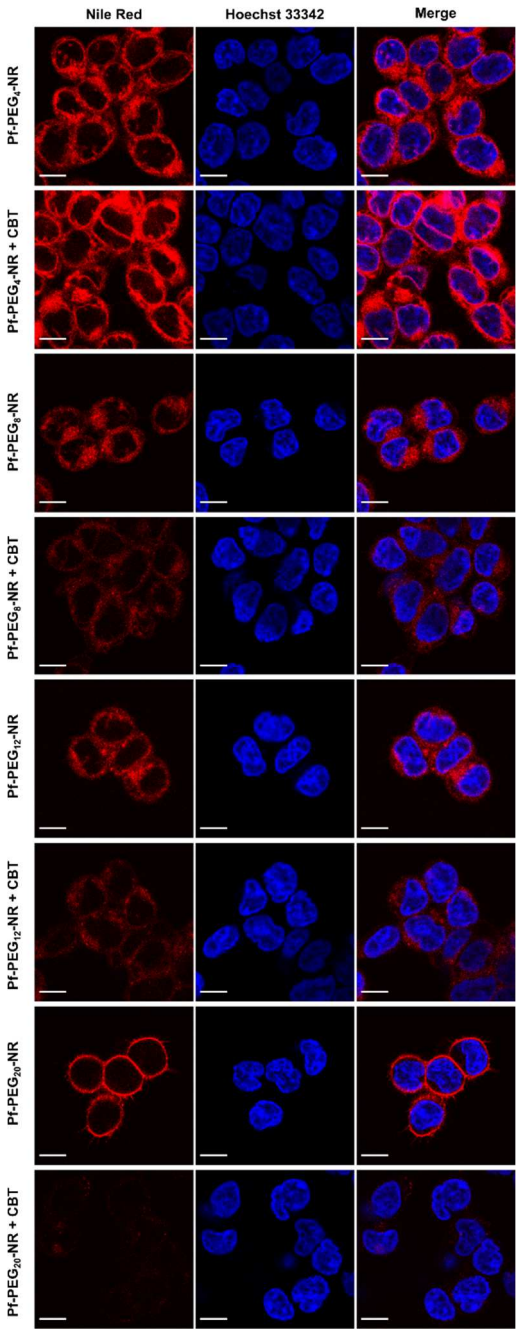

Figure 3. Confocal microscopy of the fluorogenic OTR ligands in living HEK293 cells overexpressing the OTR under no-wash conditions. Non-specific binding is evaluated in the presence of a 200-fold excess of the non-fluorescent OTR ligand carbetocin (CBT). Concentrations: OTR ligands 10 nM, CBT 2 µM. The cells were incubated with fluorescent ligands for 20 min at 37 °C prior to the imaging. Fluorescence of Nile Red (570 – 630 nm) is shown in red, nuclei stained with Hoechst 33342 are shown in blue. Scale bars, 10 µm.

Ratiometric Confocal Microscopy Studies. To demonstrate the utility of the fluorogenic NR-based ligands for selective probing of the receptor microenvironment, ratiometric confocal microscopy experiments were performed under wash-free conditions on living HEK-OTR cells. We used a ratiometry-based fluorescence sensing, which is insensitive to the concentration of the ligand and the expression level of the receptor, facilitating quantitative analysis of fluorescence data.[19,47] Upon excitation with the 488 nm laser, the emitted light was collected separately in two channels, referred

here as the "green" (500-600 nm) and the "red" (600-700 nm) channels. Taking into account the positive fluorescence solvatochromism of Nile Red derivatives, one could expect that a stronger fluorescence in the "red" channel indicates a more polar (or less hydrophobic) microenvironment. Accordingly, a stronger fluorescence in the "green" channel indicates less polar (or more hydrophobic) microenvironment of the fluorophore (Figure 4A). In other words, the relative "red-to-green" ratio (RTG) can be used as a simple quantitative measure of the polarity of the microenvironment of the probe.

The observed RTG values differed dramatically for Pf-PEG$_{20}$-NR and the other OTR ligands with shorter linker length in the cellular context (Figure 4B-E). In living cells, the fluorophore of Pf-PEG$_{20}$-NR was surrounded by a strongly apolar microenvironment with a mean RTG value of 0.90 ± 0.04. For comparison, the observed mean RTG value of the membrane probe NR12S[30] (Figure 5A) localized in the outer leaflet of the plasma membrane was 0.73 ± 0.01. In contrast, the fluorescence of the Nile Red derivatives with shorter PEG linkers was shifted to the red with mean RTG values above 1.5. These data confirmed the conclusion drawn from the confocal microscopy images (Figure 3) about the undesired penetration of the probes with PEG lengths of 4, 8 and 12 inside the cell. It also suggested that the mentioned probes reside within intracellular membrane compartment of different composition compared to the outer leaflet of the cell membrane. The observed higher RTG values inside the cells for the probes with short PEG linkers reflect higher polarity of the intracellular membranes compared to the plasma membranes, previously reported by cell permeable solvatochromic probes.[48] On the other hand, Pf-PEG$_{20}$-NR does not penetrate inside the cell and is localized within a rather apolar environment, likely within the lipid bilayer in the vicinity of the receptor.

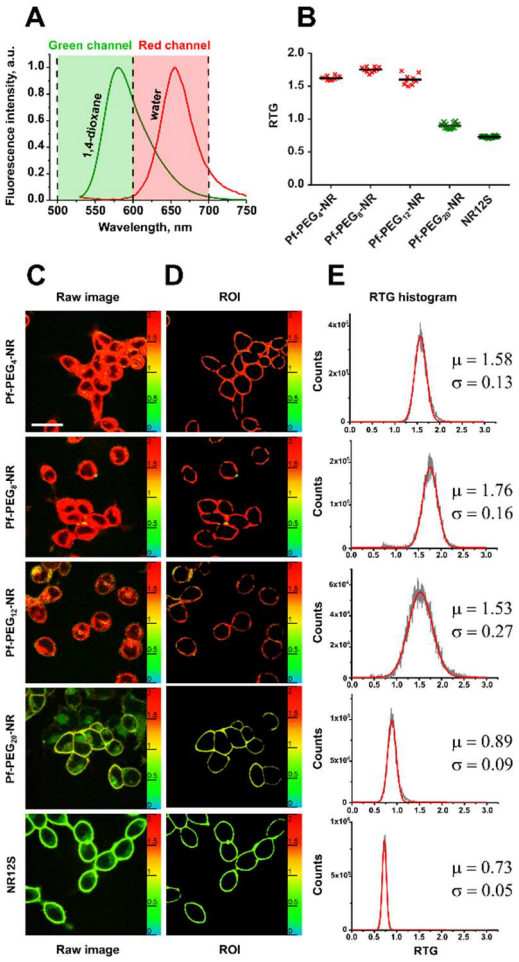

Figure 4. Ratiometric confocal microscopy imaging with NR-based probes. a) Uncorrected normalized fluorescence spectra of Pf-PEG_4-NR in 1,4-dioxane and water with the indication of the green and the red channels used for the calculation of the RTG ratio. b) Comparison of mean RTG values resulted from the cellular staining for different probes. Data from two biological replicates, five to seven images per condition were analyzed. c) Imaging of living HEK293 cells overexpressing the OTR with the NR conjugates and NR12S[30] (*vide infra*) under no-wash conditions. The pseudocolor scale indicates RTG values of the Nile Red fluorescence. Scale bar, 30 µm. d) ROI used for quantification. e) Frequencies (grey) and adjusted normal distributions (red) of RTG values for the ROI presented in d).

To further address the question of the localization of the fluorophore in Pf-PEG_{20}-NR bound to the OTR, we compared it with the previously reported specific peptidic OTR ligand CBT-NR[34] lacking a flexible spacer between the fluorophore and the pharmacophore (Figure 5A). Although the structure of OTR bound to a peptidic ligand has not been solved yet, the recently published crystal structure of the OTR bound to a non-peptidic antagonist provides insights on the structure of the orthosteric binding pocket of the receptor. The study demonstrated that the OTR possesses an enlarged orthosteric binding site, situated at the extracellular part of the receptor and comprised of a polar solvent-exposed interaction surface and a hydrophobic crevice.[49] In such case, it is highly unlikely that the fluorophore in CBT-NR–OTR complex could be deeply embedded into the cell membrane. Most probably, the fluorophore in CBT-NR bound to the OTR resides within its large ligand-binding pocket or an allosteric binding site. We obtained a mean RTG value of 1.13 ± 0.02 for CBT-NR bound to the OTR (Figure 5B), which indicates that the fluorophore resides within a more polar environment comparing to that of the bulk cellular membrane reported by NR12S (mean RTG value of 0.73 ± 0.01). This result is in line with the hypothesis that the fluorophore in CBT-NR is not embedded into the membrane. For the non-peptidic OTR ligand Pf-PEG_{20}-NR, its microenvironment characterized by a mean RTG value of 0.90 ± 0.04, was different from that of the 'linkerless' OTR ligand CBT-NR. The mean RTG value of Pf-PEG_{20}-NR also appeared to be different from the membrane-averaged RTG value measured with the membrane probe NR12S (0.73 ± 0.01), indicating that Pf-PEG_{20}-NR could uniquely probe the local lipid bilayer surrounding the transmembrane receptor.

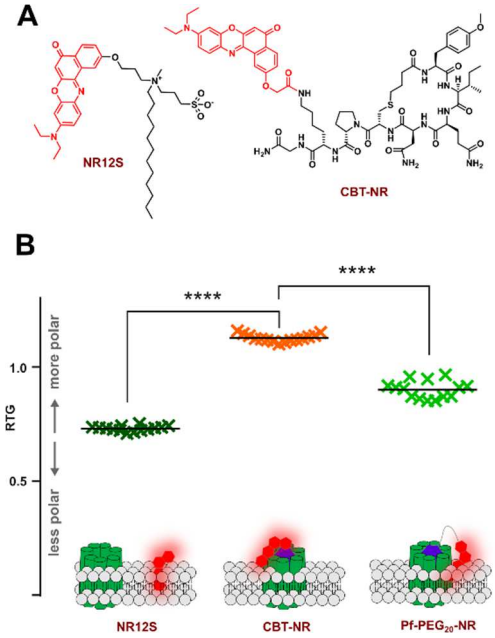

Figure 5. Evaluation of the polarity of the local microenvironment of the OTR. a) Chemical structure of the membrane probe NR12S[30] and the peptidic OTR ligand CBT-NR[34]. b) Comparison of mean RTG values resulted from the cellular staining for different probes. NR12S reports the properties of the bulk membrane, CBT-NR reports from a receptor ligand-binding pocket or an allosteric binding site, Pf-PEG20-NR reports from the lipid bilayer in the vicinity of the receptor. Data from two biological replicates, seven images per condition were analyzed. Statistics: one-way ANOVA with Tukey's multiple comparison test (confidence interval 99%, adjusted p values: **** < 0.0001).

If the suggestion that Pf-PEG$_{20}$-NR resided in the lipid bilayer in the vicinity of the receptor was correct, the probe should report changes in the lipid composition of the cell membrane. Klymchenko et al.[30] showed that the membrane probe NR12S displayed a red shift of fluorescence spectrum upon treatment of living U87MG cells with methyl-β-cyclodextrin (MβCD). One of the known effects of MβCD treatment is cholesterol depletion, which would decrease the number and size of the cholesterol-rich ordered (L_O) microdomains in the plasma membrane.[50] We first evaluated the fluorescence properties of NR12S and Pf-PEG$_4$-NR in DOPC and DOPC/cholesterol (2:1) LUVs. As expected, the fluorescence of both NR derivatives was red-shifted in LUVs without cholesterol (Supplementary Figure S1). We then performed MβCD treatment in our cell line (HEK293) stably overexpressing the OTR in the presence of membrane-specific probes NR12S or Pf-PEG$_{20}$-NR. The emission of NR12S shifted slightly to the red upon MβCD treatment as follows from the increase of its mean RTG value from 0.73 ± 0.01 to 0.79 ± 0.02 (Figure 6). Under the same condition, the receptor-bound probe Pf-PEG$_{20}$-NR displayed a similar trend by increasing its mean RTG value from 0.90 ± 0.04 to 0.98 ± 0.08. The unidirectional shift of the mean RTG for the both probes supports out suggestion that the fluorophore of the Pf-PEG$_{20}$-NR probe reaches the membrane and reports the changes of local lipid environment of the receptor.

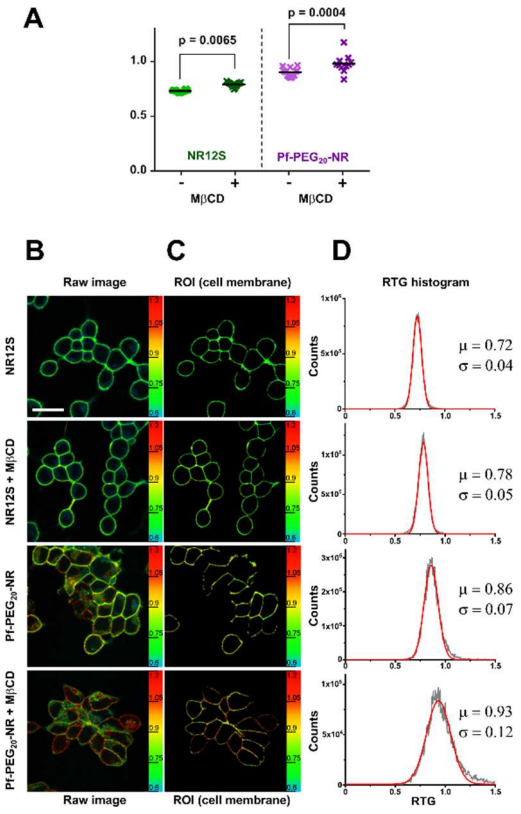

Figure 6. Influence of the MβCD treatment on the local microenvironment of the OTR. a) Comparison of mean RTG values resulted from the cellular staining with Pf-PEG$_{20}$-NR and NR12S before and after the MβCD treatment. Data from two biological replicates, seven images per condition were analyzed. Statistics: one-way ANOVA with Tukey's multiple comparison test (confidence interval 99%). b) Imaging of living HEK293 cells overexpressing the OTR stained Pf-PEG$_{20}$-NR and NR12S under no-wash conditions before and after the MβCD treatment. The pseudocolor scale indicates RTG values of the Nile Red fluorescence. Scale bar, 30 μm. c) ROI used for quantification. d) Frequencies (grey) and adjusted normal distributions (red) of RTG values for the ROI presented in c).

CONCLUSIONS

In this work, we developed first environment-sensitive antagonist probes for the oxytocin GPCR by covalently tethering the Nile Red fluorophore to a non-peptidic OTR antagonist. Our best probe Pf-PEG$_{20}$-NR featured a combination of excellent fluorogenicity, strong positive solvatochromism and negligible non-specific binding to lipid membranes and serum proteins. It enabled fluorescence imaging of the OTR in cultured cells under wash-free conditions with negligible background fluorescence. The new conjugate also enabled direct fluorescence ratiometric probing of the local plasma membrane microenvironment in the proximity to the transmembrane receptor. To date, very few methods are available for studying lipid heterogeneity of the cell membrane in space and time. None of these methods has been used for the analysis of lipid bilayer in the vicinity of an unmodified G protein-coupled receptor. In this context, Pf-PEG$_{20}$-NR represents the first fluorescent GPCR ligand able to probe the microenvironment of the unmodified receptor. The probe design presented in this work could be easily expanded for studies of other membrane receptors.

METHODS

Fluorescence Confocal Microscopy

Cell lines and culture conditions. HEK293 cells stably overexpressing the OTR were cultured in Eagle's minimal essential medium (MEM, Invitrogen 21090) with 10% FBS, 100 U mL^{-1} of penicillin, 100 µg mL^{-1} of streptomycin, 2 mM of glutamine and 500 µg mL^{-1} of G418 at 37 °C in a humidified 5% CO_2 atmosphere. 70–80% cell confluence was maintained by removal of a portion of the culture and replacement with fresh medium twice a week. Cells were seeded into 35 mm ibiTreat µ-dish (IBiDi) at 40 000 cells per dish 3 days before imaging.

Live-cell no-wash OTR imaging. The culture medium was removed, the cells were washed with PBS and incubated with a 1 µg mL^{-1} solution of Hoechst 33342 in MEM for 15 min at 37 °C. The medium was removed, the cells were washed with PBS and a 10 nM solution of the studied probe in PBS or a mixture of 10 nM of the studied probe and 2 µM of carbetocin in PBS were added. The cells were incubated for 20 min at 37 °C prior to the imaging. The imaging was performed at 22 °C. Nile Red was excited with a 488 nm 10 mW laser at 80% intensity and detected at 570 – 630 nm. Hoechst 33342 was excited with a 405 nm 25 mW laser at 10% intensity and detected at 430 – 480 nm. The pinhole was set to 1 airy unit. The images were acquired at 1.5x magnification as a mean of 2 scans in 1024x1024 size. All images were processed with ImageJ 1.53e. An additional 2x magnification was applied upon processing. The same brightness and contrast parameters for the Nile Red channel were applied to all the images.

MβCD treatments. The culture medium was removed, the cells were washed with Opti-MEM (no phenol red) and incubated with a freshly prepared 5 mM solution of MβCD in Opti-MEM (no phenol red) for 30 min at 37 °C. The cells were then washed with Opti-MEM (no phenol red) and incubated with corresponding probes.

Ratiometric confocal microscopy imaging. The culture medium was removed, the cells were washed with Opti-MEM (no phenol red) and incubated with 20 nM solutions of the studied probes in Opti-MEM (no phenol red) for 20 min at 37 °C. The imaging was performed at 22 °C. Nile Red was excited with a 488 nm 10 mW laser at 30% (Pf-PEG_4-NR), 50% (Pf-PEG_8-NR) or 80% (for other probes). The fluorescence was collected from 500 nm to 600 nm ("green" channel C1) and from 600 nm to 700 nm ("red" channel C2). Images were acquired at 1.5x magnification in 512x512 size, 20 scans in each channel. All images were processed with ImageJ 1.53e. Fluorescence intensity in each channel was averaged using z-stack projection. The mean of grey values of background signal was subtracted in both channels. RTG values of the cell membrane were calculated by dividing the mean of grey values in the obtained masks in C2 by that in C1. The ratiometric confocal microscopy images were generated using the ImageJ macros "Ratio Intensity color Version 2.5" (developed by Romain Vauchelles, UMR 7213) that divides background-subtracted image of the "red" channel bybackground-subtracted image of the "green" channel. For each pixel, a pseudocolor scale is used for coding the RTG ratio.

ASSOCIATED CONTENT

Supporting Information Available: Synthetic procedures, Absorption and Steady-State Fluorescence Measurements, Functional Characterization of the OTR ligands. This material is available free of charge *via* the Internet.

AUTHOR INFORMATION

Corresponding authors

Iuliia A. Karpenko - Laboratoire d'Innovation Thérapeutique UMR7200, CNRS/Université de Strasbourg, Strasbourg Drug Discovery and Development Institute (IMS), 74 route du Rhin, 67401 Illkirch-Graffenstaden, France; orcid.org/0000-0002-7633-3691; Email: i.karpenko@unistra.fr

Dominique Bonnet - Laboratoire d'Innovation Thérapeutique UMR7200, CNRS/Université de Strasbourg, Strasbourg Drug Discovery and Development Institute (IMS), 74 route du Rhin, 67401 Illkirch-Graffenstaden, France; orcid.org/0000-0002-8252-9199; Email: dominique.bonnet@unistra.fr

Authors

Fabien Hanser - Laboratoire d'Innovation Thérapeutique UMR7200, CNRS/Université de Strasbourg, Strasbourg Drug Discovery and Development Institute (IMS), 74 route du Rhin, 67401 Illkirch-Graffenstaden, France;

Claire Marsol - Laboratoire d'Innovation Thérapeutique UMR7200, CNRS/Université de Strasbourg, Strasbourg Drug Discovery and Development Institute (IMS), 74 route du Rhin, 67401 Illkirch-Graffenstaden, France and Platform of Integrative Chemical Biology of Strasbourg (PCBIS), LabEx MEDALIS, UMS 3286 CNRS/Université de Strasbourg, ESBS Pôle API, Bld Sébastien Brant, 67412 Illkirch-Graffenstaden, France

Christel Valencia - Platform of Integrative Chemical Biology of Strasbourg (PCBIS), UMS 3286 CNRS/Université de Strasbourg, ESBS Pôle API, Strasbourg Drug Discovery and Development Institute (IMS), Bld Sébastien Brant, 67412 Illkirch-Graffenstaden, France

Pascal Villa - Platform of Integrative Chemical Biology of Strasbourg (PCBIS), UMS 3286 CNRS/Université de Strasbourg, ESBS Pôle API, Strasbourg Drug Discovery and Development Institute (IMS), Bld Sébastien Brant, 67412 Illkirch-Graffenstaden, France

Andrey S. Klymchenko - Laboratoire de Bioimagerie et Pathologies, UMR 7021 CNRS/Université de Strasbourg, 74 route du Rhin, 67401 Illkirch-Graffenstaden, France; orcid.org/0000-0002-2423-830X

Notes

# I.A. Karpenko and D. Bonnet contributed equally to this work.

The authors declare no competing financial interest.

ACKNOWLEDGEMENTS

This work of the Strasbourg Drug Discovery and Development Institute (IMS), as part of the Interdisciplinary Thematic Institute (ITI) 2021-2028 program of the University of Strasbourg, CNRS and Inserm, was supported by IdEx Unistra (ANR-10-IDEX-0002) and by SFRI-STRAT'US project (ANR-20-SFRI-0012) under the framework of the French Investments for the Future Program. F.H. was supported by a fellowship from Pierre Fabre and the LabEx MEDALIS (ANR-10-LABX-0034). We are grateful to S. Gioria and A. Obrecht (Plate-forme de Chimie Biologique Intégrative de Strasbourg, UMS3286) for the assistance in cell culture experiments, D. Garnier and E. Oliva (PACSI platform

GDS3670) for mass spectrometry and NMR spectroscopy and D. Dziuba for fruitful suggestions and proofreading the manuscript.

References

(1) Hauser, A. S., Attwood, M. M., Rask-Andersen, M., Schiöth, H. B., and Gloriam, D. E. (2017) Trends in GPCR drug discovery: new agents, targets and indications. *Nat Rev Drug Discov 16*, 829–842.
(2) Santos, R., Ursu, O., Gaulton, A., Bento, A. P., Donadi, R. S., Bologa, C. G., Karlsson, A., Al-Lazikani, B., Hersey, A., Oprea, T. I., and Overington, J. P. (2017) A comprehensive map of molecular drug targets. *Nat Rev Drug Discov 16*, 19–34.
(3) Davenport, A. P., Scully, C. C. G., de Graaf, C., Brown, A. J. H., and Maguire, J. J. (2020) Advances in therapeutic peptides targeting G protein-coupled receptors. *Nat Rev Drug Discov 19*, 389–413.
(4) Sriram, K., and Insel, P. A. (2018) G Protein-Coupled Receptors as Targets for Approved Drugs: How Many Targets and How Many Drugs? *Mol Pharmacol 93*, 251–258.
(5) Hilger, D., Masureel, M., and Kobilka, B. K. (2018) Structure and dynamics of GPCR signaling complexes. *Nat Struct Mol Biol 25*, 4–12.
(6) Weis, W. I., and Kobilka, B. K. (2018) The Molecular Basis of G Protein–Coupled Receptor Activation. *Annu. Rev. Biochem. 87*, 897–919.
(7) Congreve, M., de Graaf, C., Swain, N. A., and Tate, C. G. (2020) Impact of GPCR Structures on Drug Discovery. *Cell 181*, 81–91.
(8) Lingwood, D., and Simons, K. (2010) Lipid Rafts As a Membrane-Organizing Principle. *Science 327*, 46–50.
(9) Sezgin, E., Levental, I., Mayor, S., and Eggeling, C. (2017) The mystery of membrane organization: composition, regulation and roles of lipid rafts. *Nat Rev Mol Cell Biol 18*, 361–374.
(10) Wiseman, D. N., Otchere, A., Patel, J. H., Uddin, R., Pollock, N. L., Routledge, S. J., Rothnie, A. J., Slack, C., Poyner, D. R., Bill, R. M., and Goddard, A. D. (2020) Expression and purification of recombinant G protein-coupled receptors: A review. *Protein Expression and Purification 167*, 105524.
(11) Wacker, D., Stevens, R. C., and Roth, B. L. (2017) How Ligands Illuminate GPCR Molecular Pharmacology. *Cell 170*, 414–427.
(12) Huber, T., and Sakmar, T. P. (2014) Chemical Biology Methods for Investigating G Protein-Coupled Receptor Signaling. *Chemistry & Biology 21*, 1224–1237.
(13) Grunbeck, A., and Sakmar, T. P. (2013) Probing G Protein-Coupled Receptor—Ligand Interactions with Targeted Photoactivatable Cross-Linkers. *Biochemistry 52*, 8625–8632.
(14) Ciruela, F., Jacobson, K. A., and Fernández-Dueñas, V. (2014) Portraying G Protein-Coupled Receptors with Fluorescent Ligands. *ACS Chem. Biol. 9*, 1918–1928.
(15) Ma, Z., Du, L., and Li, M. (2014) Toward Fluorescent Probes for G-Protein-Coupled Receptors (GPCRs): Miniperspective. *J. Med. Chem. 57*, 8187–8203.
(16) Soave, M., Briddon, S. J., Hill, S. J., and Stoddart, L. A. (2020) Fluorescent ligands: Bringing light to emerging GPCR paradigms. *Br J Pharmacol 177*, 978–991.
(17) Tian, H., Fürstenberg, A., and Huber, T. (2017) Labeling and Single-Molecule Methods To Monitor G Protein-Coupled Receptor Dynamics. *Chem. Rev. 117*, 186–245.
(18) Demchenko, A. P., Mély, Y., Duportail, G., and Klymchenko, A. S. (2009) Monitoring Biophysical Properties of Lipid Membranes by Environment-Sensitive Fluorescent Probes. *Biophysical Journal 96*, 3461–3470.
(19) Klymchenko, A. S. (2017) Solvatochromic and Fluorogenic Dyes as Environment-Sensitive Probes: Design and Biological Applications. *Acc. Chem. Res. 50*, 366–375.
(20) Dijkman, P. M., and Watts, A. (2015) Lipid modulation of early G protein-coupled receptor signalling events. *Biochimica et Biophysica Acta (BBA) - Biomembranes 1848*, 2889–2897.
(21) Mondal, S., Khelashvili, G., Johner, N., and Weinstein, H. (2014) How the Dynamic Properties and Functional Mechanisms of GPCRs Are Modulated by Their Coupling to the Membrane Environment,

in *G Protein-Coupled Receptors - Modeling and Simulation* (Filizola, M., Ed.), pp 55–74. Springer Netherlands, Dordrecht.
(22) Gahbauer, S., and Böckmann, R. A. (2020) Comprehensive Characterization of Lipid-Guided G Protein-Coupled Receptor Dimerization. *J. Phys. Chem. B 124*, 2823–2834.
(23) Gahbauer, S., and Böckmann, R. A. (2016) Membrane-Mediated Oligomerization of G Protein Coupled Receptors and Its Implications for GPCR Function. *Front. Physiol. 7,* 494.
(24) Bolivar, J. H., Muñoz-García, J. C., Castro-Dopico, T., Dijkman, P. M., Stansfeld, P. J., and Watts, A. (2016) Interaction of lipids with the neurotensin receptor 1. *Biochimica et Biophysica Acta (BBA) - Biomembranes 1858*, 1278–1287.
(25) Yoshida, K., Nagatoishi, S., Kuroda, D., Suzuki, N., Murata, T., and Tsumoto, K. (2019) Phospholipid Membrane Fluidity Alters Ligand Binding Activity of a G Protein-Coupled Receptor by Shifting the Conformational Equilibrium. *Biochemistry 58*, 504–508.
(26) Becher, A., and McIlhinney, R. A. J. (2005) Consequences of lipid raft association on G-protein-coupled receptor function. *Biochemical Society Symposia* (McIlhinney, J., and Hooper, N., Eds.) *72*, 151–164.
(27) Levental, I., Levental, K. R., and Heberle, F. A. (2020) Lipid Rafts: Controversies Resolved, Mysteries Remain. *Trends in Cell Biology 30*, 341–353.
(28) Dietrich, C., Bagatolli, L. A., Volovyk, Z. N., Thompson, N. L., Levi, M., Jacobson, K., and Gratton, E. (2001) Lipid Rafts Reconstituted in Model Membranes. *Biophysical Journal 80*, 1417–1428.
(29) Jin, L., Millard, A. C., Wuskell, J. P., Dong, X., Wu, D., Clark, H. A., and Loew, L. M. (2006) Characterization and Application of a New Optical Probe for Membrane Lipid Domains. *Biophysical Journal 90*, 2563–2575.
(30) Kucherak, O. A., Oncul, S., Darwich, Z., Yushchenko, D. A., Arntz, Y., Didier, P., Mély, Y., and Klymchenko, A. S. (2010) Switchable Nile Red-Based Probe for Cholesterol and Lipid Order at the Outer Leaflet of Biomembranes. *J. Am. Chem. Soc. 132*, 4907–4916.
(31) Danylchuk, D. I., Moon, S., Xu, K., and Klymchenko, A. S. (2019) Switchable Solvatochromic Probes for Live-Cell Super-resolution Imaging of Plasma Membrane Organization. *Angew. Chem. Int. Ed. 58*, 14920–14924.
(32) Klymchenko, A. S., and Kreder, R. (2014) Fluorescent Probes for Lipid Rafts: From Model Membranes to Living Cells. *Chemistry & Biology 21*, 97–113.
(33) Buenaventura, T., Bitsi, S., Laughlin, W. E., Burgoyne, T., Lyu, Z., Oqua, A. I., Norman, H., McGlone, E. R., Klymchenko, A. S., Corrêa, I. R., Walker, A., Inoue, A., Hanyaloglu, A., Grimes, J., Koszegi, Z., Calebiro, D., Rutter, G. A., Bloom, S. R., Jones, B., and Tomas, A. (2019) Agonist-induced membrane nanodomain clustering drives GLP-1 receptor responses in pancreatic beta cells. *PLoS Biol* (Titchenell, P., Ed.) *17*, e3000097.
(34) Karpenko, I. A., Kreder, R., Valencia, C., Villa, P., Mendre, C., Mouillac, B., Mély, Y., Hibert, M., Bonnet, D., and Klymchenko, A. S. (2014) Red Fluorescent Turn-On Ligands for Imaging and Quantifying G Protein-Coupled Receptors in Living Cells. *ChemBioChem 15*, 359–363.
(35) Darwich, Z., Klymchenko, A. S., Dujardin, D., and Mély, Y. (2014) Imaging lipid order changes in endosome membranes of live cells by using a Nile Red-based membrane probe. *RSC Adv. 4*, 8481–8488.
(36) Kreder, R., Pyrshev, K. A., Darwich, Z., Kucherak, O. A., Mély, Y., and Klymchenko, A. S. (2015) Solvatochromic Nile Red Probes with FRET Quencher Reveal Lipid Order Heterogeneity in Living and Apoptotic Cells. *ACS Chem. Biol. 10*, 1435–1442.
(37) Brown, A., Brown, T. B., Calabrese, A., Ellis, D., Puhalo, N., Ralph, M., and Watson, L. (2010) Triazole oxytocin antagonists: Identification of an aryloxyazetidine replacement for a biaryl substituent. *Bioorganic & Medicinal Chemistry Letters 20*, 516–520.
(38) Karpenko, I. A., Margathe, J.-F., Rodriguez, T., Pflimlin, E., Dupuis, E., Hibert, M., Durroux, T., and Bonnet, D. (2015) Selective Nonpeptidic Fluorescent Ligands for Oxytocin Receptor: Design, Synthesis, and Application to Time-Resolved FRET Binding Assay. *J. Med. Chem. 58*, 2547–2552.

(39) Briggs, M. S. J., Bruce, I., Miller, J. N., Moody, C. J., Simmonds, A. C., and Swann, E. (1997) Synthesis of functionalised fluorescent dyes and their coupling to amines and amino acids. *J. Chem. Soc., Perkin Trans. 1* 1051–1058.
(40) Martin-Brown, S. A., Fu, Y., Saroja, G., Collinson, M. M., and Higgins, D. A. (2005) Single-Molecule Studies of Diffusion by Oligomer-Bound Dyes in Organically Modified Sol−Gel-Derived Silicate Films. *Anal. Chem. 77*, 486–494.
(41) Kashida, H., and Asanuma, H. (2012) Preparation of supramolecular chromophoric assemblies using a DNA duplex. *Phys. Chem. Chem. Phys. 14*, 7196.
(42) Mukherjee, S., Raghuraman, H., and Chattopadhyay, A. (2007) Membrane localization and dynamics of Nile Red: Effect of cholesterol. *Biochimica et Biophysica Acta (BBA) - Biomembranes 1768*, 59–66.
(43) Greenspan, P., Mayer, E. P., and Fowler, S. D. (1985) Nile red: a selective fluorescent stain for intracellular lipid droplets. *The Journal of Cell Biology 100*, 965–973.
(44) Sackett, D. L., and Wolff, J. (1987) Nile red as a polarity-sensitive fluorescent probe of hydrophobic protein surfaces. *Analytical Biochemistry 167*, 228–234.
(45) Lampe, J. N., Fernandez, C., Nath, A., and Atkins, W. M. (2008) Nile Red Is a Fluorescent Allosteric Substrate of Cytochrome P450 3A4 †. *Biochemistry 47*, 509–516.
(46) Black, S. L., Stanley, W. A., Filipp, F. V., Bhairo, M., Verma, A., Wichmann, O., Sattler, M., Wilmanns, M., and Schultz, C. (2008) Probing lipid- and drug-binding domains with fluorescent dyes. *Bioorganic & Medicinal Chemistry 16*, 1162–1173.
(47) Demchenko, A. P. (2010) The Concept of λ-Ratiometry in Fluorescence Sensing and Imaging. *J Fluoresc 20*, 1099–1128.
(48) Ashoka, A. H., Ashokkumar, P., Kovtun, Y. P., and Klymchenko, A. S. (2019) Solvatochromic Near-Infrared Probe for Polarity Mapping of Biomembranes and Lipid Droplets in Cells under Stress. *J. Phys. Chem. Lett. 10*, 2414–2421.
(49) Waltenspühl, Y., Schöppe, J., Ehrenmann, J., Kummer, L., and Plückthun, A. (2020) Crystal structure of the human oxytocin receptor. *Sci. Adv. 6*, eabb5419.
(50) Mahammad, S., and Parmryd, I. (2015) Cholesterol Depletion Using Methyl-β-cyclodextrin, in *Methods in Membrane Lipids* (Owen, D. M., Ed.), pp 91–102. Springer New York, New York, NY.